

INORGANIC SYNTHESIS  
AND INDUSTRIAL INORGANIC CHEMISTRY

## Synthesis of Aluminum Oxides with Controlled Textural and Strength Parameters

A. S. Zaguzin<sup>a,\*</sup>, A. V. Romanenko<sup>a</sup>, and M. V. Bukhtiyarova<sup>a</sup>

<sup>a</sup> Borekov Institute of Catalysis, Siberian Branch of Russian Academy of Sciences, Novosibirsk, 630090 Russia

\*e-mail: zaguzin@catalysis.ru

Received October 26, 2019; revised March 13, 2020; accepted April 9, 2020

**Abstract**—The effect of a number of burn out additives introduced into the composition of pastes prepared on the basis of aluminum hydroxide, Pural SCF-55, and the modes of sample calcination on the texture and strength parameters of the obtained aluminum oxides has been investigated. The additives are represented by three types of carbon blacks: acetylene, Vulcan XC-72, and Katjenblack EC-300J, as well as ultrafine diamonds, oxidized graphite, egg white, and bovine albumin. It is shown that the introduction of burn out additives affects both the mesoporous and macroporous structure of the support and leads to the formation of transport pores up to 10 μm in size. It has been established that calcining the formed aluminum hydroxide granules, including the considered carbon blacks, in air at 600°C with a preliminary rise in temperature to 450°C in an argon atmosphere makes it possible to obtain Al<sub>2</sub>O<sub>3</sub> with higher crushing strength.

**Keywords:** aluminum oxide, carbon, carbon black, burn-out additives, pseudoboehmite

**DOI:** 10.1134/S1070427220080029

Aluminum oxides are widely used as sorbents and desiccants. The share of their consumption in the composition of catalyst components is steadily increasing, primarily as carriers for oil refining processes such as hydrocracking, reforming, hydrotreating, as well as for the dehydrogenation of light hydrocarbons. This fact is due to the possibility of the targeted formation of various modifications of aluminum oxide ( $\gamma$ -,  $\eta$ -,  $\theta$ -Al<sub>2</sub>O<sub>3</sub>, etc.) with the required textural and strength parameters and a given surface state, which ensure the production of effective catalysts (activity, selectivity, thermal, corrosion resistance) for the developed processes.

The nature of chemical processes involving supported catalysts is largely determined by the porous structure of the used support, which can be represented by micro-, meso- and macropores. Conventionally, micro- and mesopores, in which the main catalytic transformations take place, include pores less than 2 and 2–50 nm in size, respectively, and macropores, are transport pores with a size of more than 50 nm [1].

In catalytic processes with the participation of “large” molecules, when a significant amount of the

active component is localized in micropores and on the surface of narrow mesopores, diffusion restrictions arise. Therefore, to increase the efficiency of catalysts, it is necessary either to develop complex techniques that reduce the amount of particles formed in narrow pores during the deposition of an active component, or to use meso- and macroporous carriers with a large mesopore size. It should be noted that in the second case, negative effects associated with a decrease in the specific surface area and strength characteristics of the catalyst may appear. Therefore, it seems relevant to research aimed at the development of oxide carriers with high specific surface area and strength with predetermined textural parameters.

According to the analysis of the literature data on the study of individual stages of preparation of aluminum oxides, the properties of various modifications of Al<sub>2</sub>O<sub>3</sub> are largely determined by the properties of the initial hydroxides [2–4]. Therefore, in the development of methods for the synthesis of aluminum oxides with specified microstructural, textural, and strength parameters, much attention is paid to the stage of

preparing hydroxides that differ in the size and morphology of particles, the type of their aggregation, and the nature and strength of the bond between the particles and their aggregates. A promising approach to the preparation of such hydroxides is hydrothermal synthesis in an autoclave at 120–200°C from mixtures of aluminum sulfate with urea and other additives in the presence of water. At the same time, the use of polyglycols [5], citric acid [6], and hexamethylenetetramine [7] as additives makes it possible, after the stage of hydroxide calcination, to synthesize aluminum oxides with a developed surface of meso- and macropores.

Another effective approach to the controlling the textural parameters is the introduction of additives into the composition of hydroxides that burn out when the samples are calcined. Organic acids [8, 9], high molecular weight alcohols [10, 11], polymer microspheres [12], microcrystalline cellulose [13], starch [14], carbon materials [10, 15, 16] and polymers [17, 18] are used as such additives. The introduction of such materials into the composition of the reaction mixture at the stage of the synthesis of hydroxides or into pastes prepared from hydroxides makes it possible to vary the ratio of the pore sizes of  $\text{Al}_2\text{O}_3$  in a wide range by varying the type of additive and the mode of calcining the support. To a large extent, when solid burn-out additives are introduced, the size of the generated pores will be determined by the shape and size of these particles and their aggregates. Thus, high-molecular alcohols and black carbon increase the size of mesopores [10], while the introduction of cellulose with an average particle size of 20 to 90  $\mu\text{m}$  promotes the development of macropores [13].

The aim of this work is to study the effect of various types of carbon-containing materials, including commercially available carbon blacks, introduced into the composition of pastes prepared on the basis of aluminum hydroxide (pseudoboehmite) Pural SCF-55 (Sasol Co.), on the textural and strength parameters of the synthesized aluminum oxides.

## EXPERIMENTAL

**Synthesis of carriers.** The commercial aluminum hydroxide powder (pseudoboehmite) Pural SCF-55, provided by Sasol (Germany), was used as a starting component for synthesis of  $\text{Al}_2\text{O}_3$  samples. The synthesis technique included the preparation of the

plastic mass, the molding of granules, followed by their drying and calcination.

Plastics for molding were prepared by mixing pseudoboehmite powder in distilled water using a laboratory screw mixer. Preparing the pastes, a peptizer and burnout additives were added to their composition.

The role of the peptizing additive is to break the contacts between the aluminum hydroxide particles. For these purposes, we used a solution of nitric acid of special purity grade in the molar ratio  $\text{HNO}_3/\text{Al}_2\text{O}_3 = 0.1$ . Burn-out additives are represented by three types of carbon blacks: thermal acetylene black (Acetylene black), furnace Vulcan (Vulcan XC-72), and furnace Katjenblack EC-300J, as well as ultradispersed diamonds and graphite oxide. Their choice is due to the fact that these carbon materials differ in the size of primary particles and their aggregates, and carbon blacks are commercially available. For comparison, in addition to carbon materials, two types of proteins were taken as burn-out additives: egg white and bovine albumin. In terms of aluminum oxide, the amount of the added additives was 1% for oxidized graphite, egg white and bovine albumin and 10% for all other additives.

The prepared pastes were loaded into a laboratory plunger extruder and pressed through a spinneret with a hole diameter of 3.0 mm. The resulting extrudates were dried for 15–20 h at room temperature in air, then for another 16 h at 110°C. In order to ensure the burnout of the introduced additives, the dried samples were calcined in a muffle furnace at 600°C for 8 h. Heating was carried out at a rate of 5 deg  $\text{min}^{-1}$  with an intermediate holding of the samples for 1 h at a temperature of 300°C. After drying in air at 110°C, individual samples were calcined in a flow reactor in an argon flow: 1 h at 300°C and 1 h at 450°C. Operations associated with a further increase in temperature were carried out in a muffle furnace in air.

*Research methods.* The textural parameters of the materials used as burn-out additives and the resulting oxide carriers were determined by physical adsorption of  $\text{N}_2$  at 77 K using an ASAP-2400 automated volumetric adsorption unit (Micromeritics Instrument Co., Norcross, GA, USA). Before analysis, the samples were kept at a pressure of  $1 \times 10^{-3}$  mmHg at a temperature of 150°C for 4 h. The calculation of the specific surface area ( $S_{\text{BET}}$ ) was conducted from the analysis of the adsorption branch of the isotherm by the Brunauer–Emmett–Teller method in the range of relative pressures of 0.05–0.20, and the total pore volume ( $V_{\Sigma}$ ) was based on the value

**Table 1.** Characteristics of burn-out additives

Burn-out additive	Specific surface area, $S_{\text{BET}}$ , $\text{m}^2 \text{g}^{-1}$	Primary particle diameter, nm
Acetylene black	51	90–190
Vulcan carbon black	210	40–140
Ultrafine diamonds	300	100–200
Katjenblack EC-300J	858	15–40
Oxidized graphite	231	100–740
Bovine albumin	–	~20
Egg white	–	~10

of  $\text{N}_2$  adsorption at  $P/P_0 = 0.98$ . The volumes of pores with sizes from 17 to 3000 Å were calculated from the adsorption ( $V_{\text{ads}}$ ) and desorption ( $V_{\text{des}}$ ) branches of the hysteresis of capillary condensation of nitrogen in accordance with the Barrett–Joyner–Halenda model. The average pore diameter ( $D_{\text{av}}$ ) was calculated as  $D_{\text{av}} (\text{Å}) = 4V_{\Sigma}/S_{\text{BET}}$ .

The mechanical crushing strength ( $P_{\text{cs}}$ ) was calculated as the ratio of the force (kg) required to break the sample granule along the generatrix between two parallel planes to the granule cross-section area  $S = DH$  ( $\text{cm}^2$ ) according to the formula  $P_{\text{cs}} (\text{kg cm}^{-3}) = NA/S$ , where  $N$  is indicator readings,  $A$  is calibration factor,  $D$  and  $H$  are grain diameter and length, respectively. In this case, the value of  $P_{\text{cs}}$  was determined as the average value of the mechanical strength, calculated when breaking at least 30 granules.

The morphological parameters of the particles of burn-out additives and the nature of the pores generated by them were evaluated by scanning electron microscopy using a scanning electron microscope (SEM) LEO-1430.

X-ray phase analysis of the samples was carried out on a Bruker D8 Advance diffractometer (Germany) in monochromatic  $\text{CuK}\alpha$  radiation ( $\lambda = 1.5418 \text{ Å}$ ) in the range of angles of  $2\theta$  5°–80°. The average size of the coherent scattering regions (CSR) was calculated using the Selyakov–Scherrer formula.

## RESULTS AND DISCUSSION

Micrographs of particles of the carbon materials used in this work, obtained by scanning electron microscopy, are shown in Fig. 1. Their comparative parameters are present in Table 1. The images (Fig. 1) give an idea of

the shape and size of primary particles, their aggregates and secondary structures. It can be seen that the primary black carbon particles are spherical. At the same time, furnace black is inferior to acetylene one in the size of such particles, but has a higher specific surface area, which is consistent with the literature data [19, 20]. The secondary structures of carbon blacks are bulky branched structures including loose agglomerates larger than 1  $\mu\text{m}$ . Oxidized graphite powders (Fig. 1d) consist of flat particles that can be more than 200  $\mu\text{m}$  in length. Ultradispersed diamonds are represented by dense bulk irregularly shaped particles ranging in size from 100 nm to 50  $\mu\text{m}$  (Fig. 1e). Primary protein globules of bovine albumin and egg white, according to manufacturers, have average sizes of about 20 and 10 nm, respectively.

The thermal stability of the used carbon blacks increases in the series Katjenblack EC-300J ( $S_{\text{BET}} = 858 \text{ m}^2 \text{g}^{-1}$ ) < Vulcan carbon black ( $210 \text{ m}^2 \text{g}^{-1}$ ) < acetylene black ( $51 \text{ m}^2 \text{g}^{-1}$ ). During the formation of alumina at the final stage of calcination in a muffle furnace, the extrudates were kept for 8 h at 600°C. This mode ensured the complete burnout of carbon black (control by the color of granules), including thermally stable acetylene black.

For all samples, the X-ray diffraction patterns (Fig. 2) exhibit peaks characteristic for the  $\gamma\text{-Al}_2\text{O}_3$  phase, and the average sizes (CSR) of primary alumina particles calculated from the peak half-width 440 are in the range of 5.1–5.7 nm.

The experimental values of the strength of the samples (Table 2), depending on the nature of the burn-out additive introduced and the mode of calcination, vary from 34 to 88  $\text{kg cm}^{-3}$ . Thus, in the air calcination mode, the most durable granules were obtained using

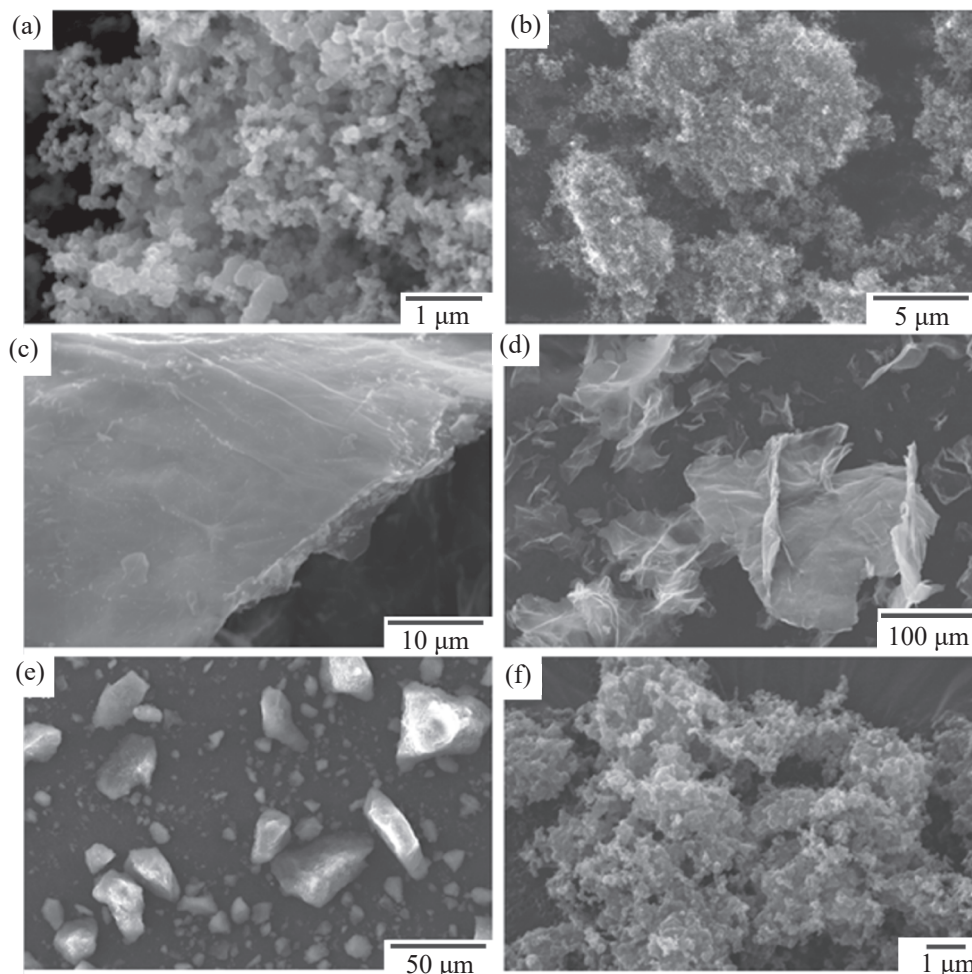


**Fig. 1.** Images of carbon material particles obtained by scanning electron microscopy: (a) acetylene black, (b) Katjenblack EC-300J, (c, d) oxidized graphite, (e) ultrafine diamonds, (f) Vulcan carbon black.

Katjenblack EC-300J carbon black. The use of carbon black with a higher thermal stability (Vulcan carbon black, acetylene black), represented by larger primary particles, led to a decrease in the strength of the sam-

ples relative to aluminum oxide prepared directly from Pural SCF-55 hydroxide. This result can be associated with the possibility of obtaining homogeneous pastes for molding with a high concentration of hydroxide mi-

**Table 2.** Comparison of strength parameters of alumina samples

Precursor to aluminum oxide	Crushing strength $P_{cs}$ , kg cm <sup>-3</sup>	
	calcining in air	intermediate calcination in Ar atmosphere
Pural SCF-55	63.7	53.0
Pural SCF-55/Katjenblack EC-300J	72.6	78.1
Pural SCF-55/Acetylene black	48.9	88.0
Pural SCF-55/Vulcan carbon black	56.8	86.9
Pural SCF-55/Ultrafine diamonds	57.1	49.9
Pural SCF-55/Oxidized graphite	52.9	52.6
Pural SCF-55/Egg white	34.4	38.1
Pural SCF-55/Bovine albumin	53.9	53.9

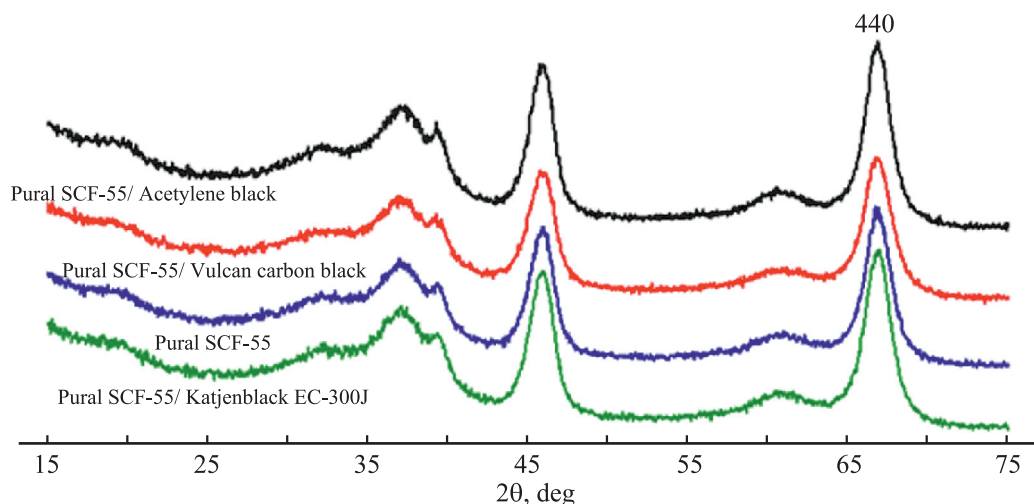


Fig. 2. (Color online) X-ray diffraction patterns of alumina samples.

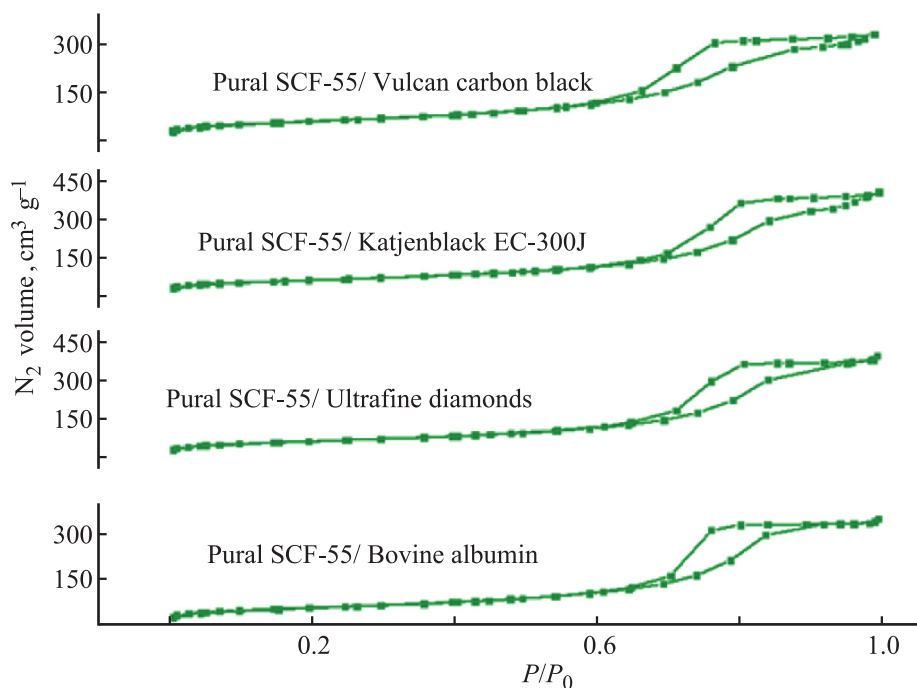
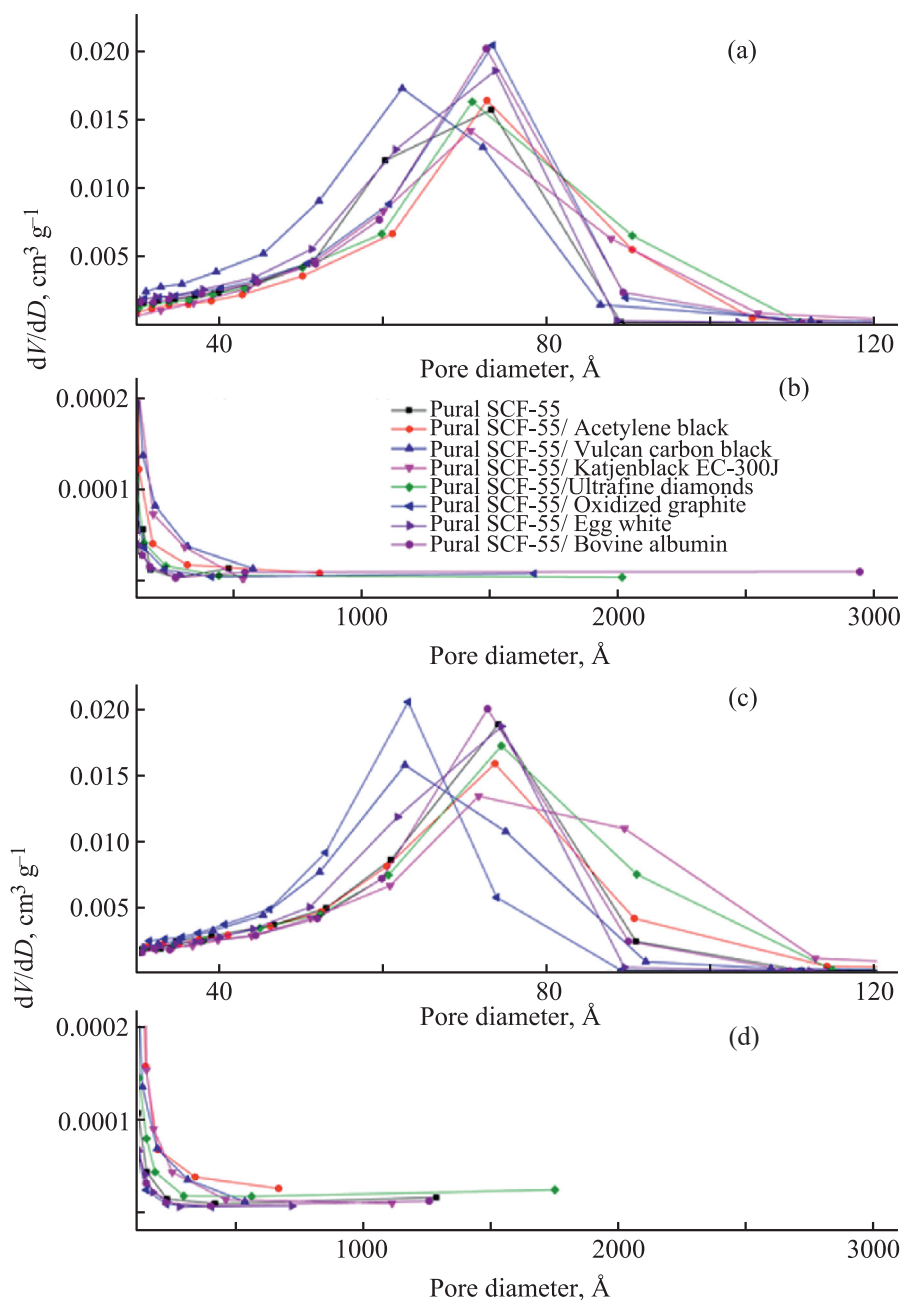


Fig. 3. Nitrogen adsorption–desorption isotherms (lower and upper curves, respectively) for  $\text{Al}_2\text{O}_3$  samples prepared by calcining granules in air.

crocrystallites in contact with each other in the presence of Katjenblack EC-300J. As mentioned above, oxidized graphite and ultradispersed diamonds consist of extended flat particles and large bulk aggregates, respectively (Fig. 1). Its burning out results in formation of larger voids, that prevents the formation of new contacts and contributes to a decrease in the strength of the samples.

Discussing the factors affecting the strength of the obtained granules, it should be taken into account

that the formation of a rigid frame of granules with a temperature increase in air is accompanied, in addition to phase transitions, by the release of the products of the interaction of the peptizer ( $\text{HNO}_3$ ) and burn-out additives with atmospheric oxygen. Using proteins in the composition of molded pastes as burn-out additives, additional problems associated with controlling the degree of swelling and partial dissolution of protein globules can arise.



**Fig. 4.** (Color online) Pore volume vs. diameter according to the data of low-temperature nitrogen adsorption: (a, c)  $D_{\text{pore}} = 30\text{--}120 \text{ \AA}$ , (b, d)  $D_{\text{pore}} = 120\text{--}3000 \text{ \AA}$ . Sample calcination mode: (a, b) in air at  $600^\circ\text{C}$  for 8 h; (c, d) in argon up to  $450^\circ\text{C}$  inclusive, then in air at  $600^\circ\text{C}$  for 8 h.

In the synthesis of a series of supports, the pre-calcining mode of the precursor of aluminum oxide in an argon flow was also used, which prevents the removal of burn-out additives when the temperature is raised to  $450^\circ\text{C}$ . In this series (Table 2), a significant increase in crushing strength is observed for all three types of commercial blacks used, Katjenblack EC-300J, acetylene black, and

Vulcan carbon black. The strength of such samples turned out to be higher than the strength of the granules calcined in air. Such an increase in strength can be due to the formation of a rigid framework of aluminum oxide before the onset of burnout of the introduced bulk carbon-containing materials at the mentioned calcination conditions at the mentioned calcination conditions.

**Table 3.** Pore size distribution for Al<sub>2</sub>O<sub>3</sub> samples prepared by calcining in air

Precursor to aluminum oxide	Surface area $S_{\text{BET}}$ , m <sup>2</sup> g <sup>-1</sup>	Pore volume $V_{\text{des}}$ , cm <sup>3</sup> g <sup>-1</sup>	Percentage of the total pore volume of their size: five intervals of average pore sizes are identified, Å					Average pore size, $D_{\text{av}}$ , Å
			30–50	50–70	70–100	100–130	>130	
Pural SCF-55	191.5	0.46	15.2	72.0	9.7	0.4	2.7	93.3
Pural SCF-55 <sup>a</sup>	221.9	0.55	10.2	23.2	61.3	0.4	4.9	98.3
Pural SCF-55/Acetylene black	190.8	0.54	12.5	11.0	69.9	1.6	5.0	111.3
Pural SCF-55/Acetylene black <sup>a</sup>	211.7	0.55	9.8	22.7	58.2	1.8	7.4	101.5
Pural SCF-55/Vulcan carbon black	228.5	0.53	12.6	48.0	30.6	1.1	6.6	90.5
Pural SCF-55/Vulcan carbon black <sup>a</sup>	215.3	0.52	11.0	46.3	36.2	1.7	4.8	94.0
Pural SCF-55/Katjenblack EC-300J	194.8	0.53	6.6	20.4	65.5	3.1	4.4	106.9
Pural SCF-55/Katjenblack EC-300J <sup>a</sup>	219.8	0.64	6.0	14.8	66.9	5.7	6.6	114.1
Pural SCF-55/Ultrafine diamonds	218.4	0.60	12.7	8.2	71.7	0.4	7.0	108.8
Pural SCF-55/Ultrafine diamonds <sup>a</sup>	226.5	0.63	8.2	19.4	63.7	0.8	7.9	108.9
Pural SCF-55/Oxidized graphite	216.9	0.55	7.7	25.4	60.7	0.4	5.9	100.2
Pural SCF-55/Oxidized graphite <sup>a</sup>	202.6	0.44	14.8	66.0	17.0	0.4	1.8	83.6
Pural SCF-55/Egg white	211.1	0.56	8.8	38.1	46.6	0.4	6.1	104.7
Pural SCF-55/Egg white <sup>a</sup>	210.0	0.51	8.6	37.7	49.4	0.4	3.9	94.6
Pural SCF-55/Bovine albumin	211.3	0.58	8.2	19.7	62.8	0.3	9.0	107.1
Pural SCF-55/Bovine albumin <sup>a</sup>	210.8	0.55	8.2	18.6	67.6	0.3	5.3	102.8

<sup>a</sup> Samples pre-calcined in argon.

Analysis of adsorption–desorption isotherms of nitrogen for Al<sub>2</sub>O<sub>3</sub> samples derived by calcining granules in air (Fig. 3), and isotherms of oxides prepared in the mode of preliminary calcining in argon, shows that all samples belong to the same type, mesoporous carriers. In this case, the hysteresis type of the isotherms of the supports prepared from Pural SCF-55 hydroxide with burn-out additives shows that these materials have cylindrical pores, i.e., correspond to the same type of hysteresis that was determined for the oxide prepared without additives. A similar result was noted in [9] using organic acids as additives.

Based on the analysis of the curves of the pore volume vs. the diameter ( $D_{\text{pore}}$ ), the introduction of burn-out additives has a significant effect on the porous structure of the obtained aluminum oxides. In such samples (Fig. 4), an increase in the amount of pores with diameter > 80 Å in

diameter occurs. An exception is Al<sub>2</sub>O<sub>3</sub> prepared by burning out Vulcan carbon black in the calcination mode in air. An increase in the amount of pores with diameter <60 Å was recorded for this sample. In this case, all changes concerning the specific surface area, total volume, and average pore diameter are observed in the mesopore region, i.e., for pores with sizes ≤50 nm (Figs. 4b, 4d). It should be noted that the analysis of the texture parameters of the samples by the method of mercury porosimetry using the AutoPore IV 9500 Micromeritics Instrument did not reveal the presence of pores in the size range of 12–15 μm.

Comparison of the results derived (Fig. 4, Table 3) showed that the textural parameters of oxides prepared from the same pastes can significantly differ depending on the calcination mode.

For oxides prepared using various burn-out additives in the air calcination mode, an increase in the specific

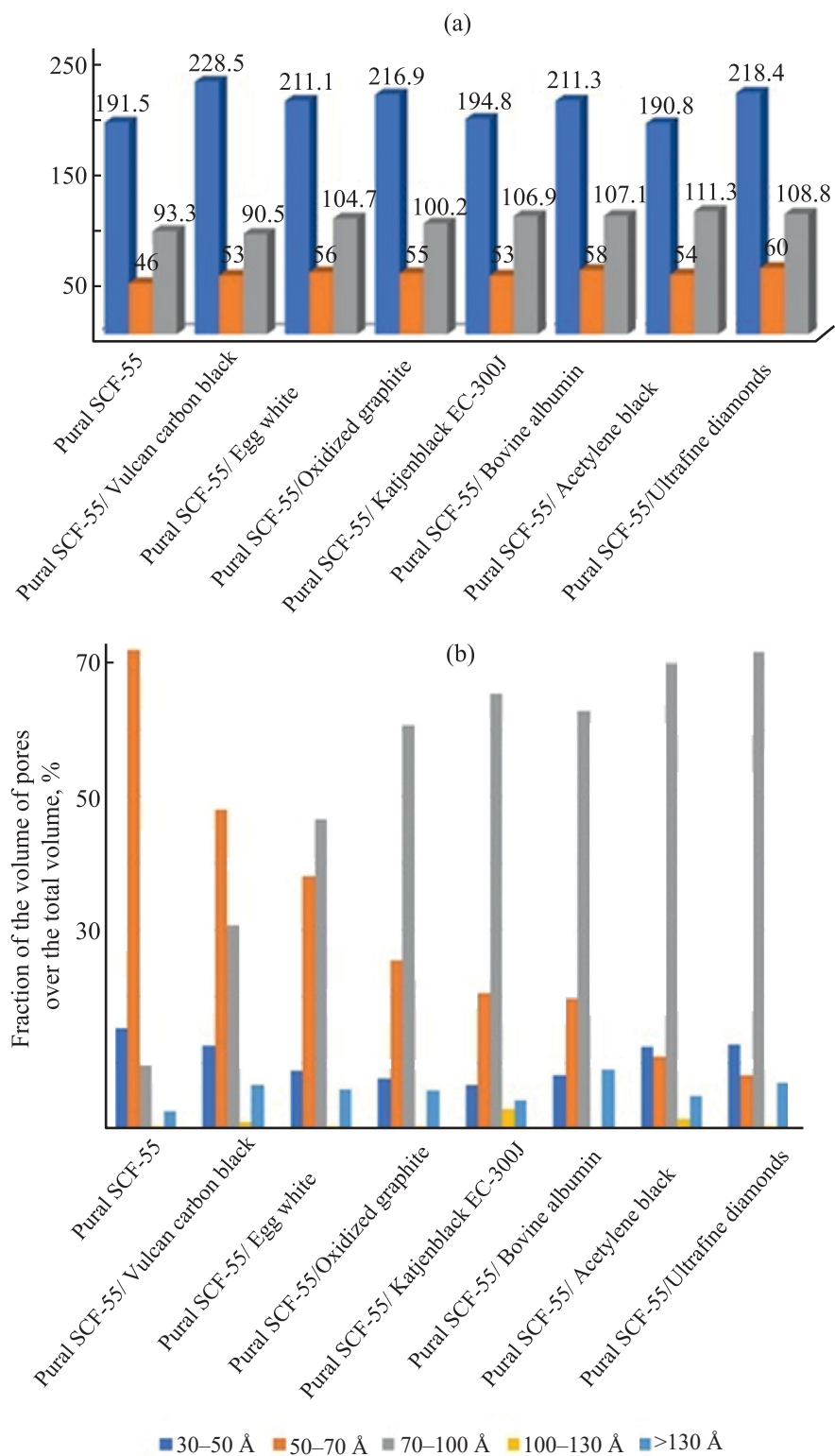


**Fig. 5.** (Color online) (a) Texture parameters and (b) pore size distribution diagram for  $\text{Al}_2\text{O}_3$  samples prepared in the air calcination mode.



surface area ( $S_{\text{BET}}$ ), volume ( $V_{\text{des}}$ ), and average size ( $D_{\text{av}}$ ) of pores occurs. In this case, the introduction of acetylene black into their composition leads to an insignificant decrease in  $S_{\text{BET}}$ , and that of Vulcan carbon black results in a decrease in  $D_{\text{av}}$  from 93.3 to 90.5 Å (Fig. 5a).

The effect of the calcination mode on the pore size distribution changes for the considered aluminum oxides was interesting to determine. Their pore space was conventionally divided into five intervals by pore size, and for each interval the percentage of the total volume was calculated (Table 3).

For clarity, oxide supports prepared by calcining in air are shown in Fig. 5b in the form of a diagram in the order of decreasing amount of pores with the size of 50–70 Å. The volume fraction of such pores decreases from 72 (Pural SCF-55 without additives) to 8% (ultradispersed diamonds as the additive). In this case, the amount of pores with a diameter of 70–100 Å increases symbolically from 10 to 72%. The introduction of burn-out additives insignificantly increases the amount of larger pores (100–130 Å). The contribution of the pores with size >130 Å (from 13 to 300 nm) increases from 3 to 9%. All samples showed a tendency towards a decrease in the amount of pores with a size of 30–50 Å from 15 (Pural SCF-55 without additives) to 7–13%, depending on the additive. However, taking into account an increase in the total pore volume of such samples, it can be assumed that the pore volume for this size range did not change.

The introduction of the stage of preliminary calcination in an argon flow during the synthesis of  $\text{Al}_2\text{O}_3$  from individual Pural SCF-55 hydroxide leads to a rise in its specific surface area, volume, and average pore diameter in addition to increasing the strength of such a support. A decrease in the volume fraction of pores of 50–70 Å from 72 to 23% as well as an increase in the amount of pores of 70–100 Å from 10 to 61% occur. For samples obtained using burn-out additives, the texture parameters change in a more complex way. Thus, the sample with the addition of Katjenblack EC-300J demonstrated a noticeable increase in pore volume (by 21%) and specific surface area (by 13%) in comparison to a similar sample not calcined in an argon flow. The sample prepared with oxidized graphite showed a 20% reduction in volume and average pore size. The textural parameters of the samples with the addition of acetylene black, ultradispersed diamonds, and Vulcan carbon

black practically do not depend on the calcination mode and are within the measurement error. Samples prepared using egg white and bovine albumin proteins showed some decrease in pore volume (<10%).

The reported data are consistent with the results of the study [10]. The authors showed that the introduction of carbon black into the boehmite composition leads to a rise in the total pore volume and average pore size in the resulting alumina with a decrease in the pore volume with a radius of 18–50 Å and a rise in the pore volume with a radius 50–100 Å.

In order to visually assess the effect of the introduction of burn-out additives, using a scanning electron microscope, micrographs of carrier granules prepared from Pural SCF-55 and various burn-out additives were obtained (Fig. 6). The granules were preliminarily split in diameter and recorded their inner side.

There are no large pores on the cut surface of a sample obtained from pure Pural SCF-55, while the introduction of burn-out additives into Pural SCF-55 promotes the appearance of macropores of different sizes up to 10 μm in alumina samples (see insets to Figs. 6b, 6c). It should be noted that the shape of the pores also changes and depends both on the size of the aggregates and on the type of added additives. In case of Katjenblack EC-300J and ultrafine diamonds, deep branched macropores are produced. The channels formed during the burnout of ultradispersed diamonds (Fig. 6b) are close in diameter to the size of dense aggregates of their initial particles (Fig. 1e). Narrow pores corresponding in shape to flat particles of graphite oxide are observed in a sample prepared with oxidized graphite (Fig. 1d). Consequently, the use of carbon materials as burn-out additives makes it possible to purposefully regulate not only the meso-, but also the macroporous structure of the samples.

The authors of [3] experimentally showed that the strength parameters of the produced aluminum oxide granules prepared from various hydroxide precursors begin to lose strength with an increase in the amount of pores larger than 50 nm. In this work, the formation of large macropores using Katjenblack EC-300J carbon black does not lead to a diminishing the strength of the resulting granules, that can be associated with its low concentration in the sample volume.

In a number of points, the approach considered in this work is inferior to other developed methods of targeted regulation of the meso- and macroporous structure of oxide carriers. In particular, the authors of [12],

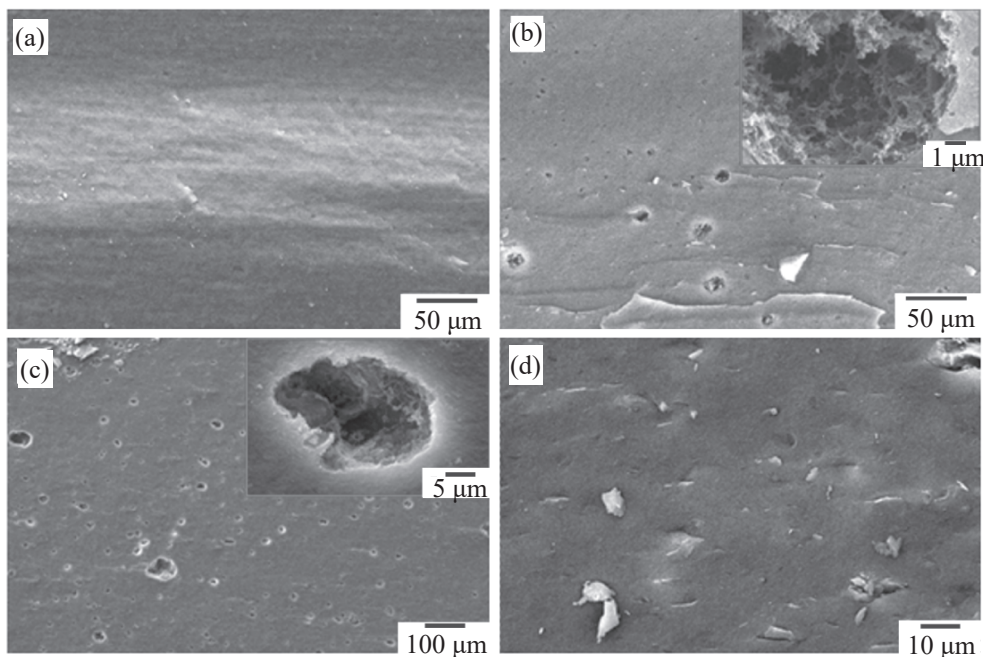


**Fig. 6.** Micrographs of the surface of the cut of the granules obtained by scanning electron microscopy. (a) Sample without additives, (b) with the addition of ultrafine diamonds, (c) Katjenblack EC-300J, (d) oxidized graphite. The oxides were calcined in air at 600°C for 8 h.

introducing into the composition of pastes the initial hydroxides of polystyrene microspheres with given sizes, manage to produce rather homogeneous composites with a controlled macropore size up to 0.5  $\mu\text{m}$ . Using carbon burn-out additives, less homogeneous materials are obtained, but with the possibility of varying the size of macropores within wider ranges. Other potential advantages of their use are the relatively low cost and commercial availability of the carbon blacks applied.

## CONCLUSIONS

Based on the results of the studies, it was found that the introduction of Katjenblack EC-300J carbon black into the composition of pastes prepared from Pural SCF-5 pseudoboehmite allows increasing the strength of the  $\text{Al}_2\text{O}_3$  prepared by 10% after calcining the molded hydroxide granules in air at 600°C. Such a result may be due to the possibility of obtaining, in the presence of amorphous carbon blacks with a developed surface, homogeneous pastes for molding with a high concentration of hydroxide microcrystallites in contact with each other. It was shown that preliminary calcination of granules to a temperature of 450°C in an argon atmosphere, i.e., under conditions preventing the

burnout of a carbon additive at the stage of formation of a rigid alumina framework leads to the production of carriers with higher crush strength for all three blacks used (Katjenblack EC-300J, acetylene, and Vulkan carbon black).

An increase in the specific surface area, pore volume, and average pore diameter occurs for oxides prepared using various burn-out additives in the air calcination mode. In this case, the introduction of Vulcan carbon black into their composition leads to a decrease in the average pore size from 93 to 90  $\text{\AA}$ , and the introduction of acetylene black, results in a slight decrease in the specific surface area. In  $\text{Al}_2\text{O}_3$  synthesized from individual Pural SCF-55, the volume fraction of mesopores 50–70  $\text{\AA}$  in size is 72%, while pores with a diameter of 70–100  $\text{\AA}$  account for 10%. Moreover, the amount of the latter rises with the introduction of burn-out additives. Burn-out additives such as acetylene black, Katjenblack EC-300J, ultrafine diamonds, bovine albumin, and graphite oxide can elevate the volume of pores with a diameter of 70–100  $\text{\AA}$  by 6–7 times. The inclusion of Katjenblack EC-300J carbon black and ultradispersed diamonds in the plastics composition allows the formation of  $\text{Al}_2\text{O}_3$  with a system of branched macropores. In this case, the voids formed during the burnout of ultradispersed

diamonds turn out to be close in diameter to the size of dense aggregates of their initial particles, and the oxides prepared using graphite oxide contain narrow pores corresponding in shape to flat particles of graphite oxide.

#### FUNDING

The work was carried out within the framework of the state assignment of the Institute of Catalysis, Siberian Branch of Russian Academy of Sciences (project AAAA-A17-117041710090-3).

#### CONFLICT OF INTEREST

The authors declare that they have no conflicts of interest requiring disclosure in this article.

#### REFERENCES

- Rouquerol, J., Rodriguez-Reinoso, F., Sing, K., S.W., and Unger K.K., *Characterization of Porous Solids III*, Amsterdam: Elsevier, 1994.
- Chukin, G.D., *Stroenie oksida alyuminiya i katalizatorov gidroobesserivaniya. Mekhanizmy reaktsii* (Structure of Aluminum Oxide and Hydrodesulfurization Catalysts. Reaction Mechanisms), Moscow: Printa, 2010.
- Dzis'ko, V.A., Vinnikova, T.S., Kefeli, L.M., and Ryzhak, I.A., *Kinetika Kataliz*, 1966, vol. VII, no. 5, pp. 859–864.
- Tregubenko, V.Y., Udras, I.E., Drozdov, V.A., and Belyi, A.S., *Russ. J. Appl. Chem.*, 2011, vol. 84, no. 1, pp. 9–16.  
<https://doi.org/10.1134/S1070427211010022>
- Li, Y., Peng, C., Li, L., and Ra, P., *J. Am. Ceram. Soc.*, 2014, vol. 97, no. 1, pp. 35–39.  
<https://doi.org/10.1111/jace.12652>
- Dong, Y., Xu, Y., Zhang, Y., Lian, X., Yi, X., Zhou, Y., and Fang, W., *Appl. Catal. A: General*, 2018, vol. 559, pp. 30–39.  
<https://doi.org/10.1016/j.apcata.2018.04.007>
- Dong, Y., Yu, X., Zhou, Y., Xu, Y., Lian, X., Yi, X., and Fang, W., *Catal. Sci. Technol.*, 2018, vol. 8, no. 7, pp. 1892–1904.  
<https://doi.org/10.1039/C7CY02621H>
- Kuznetsova, T.R. and Barkatina, E.N., *Kolloid. Zh.*, 1990, vol. 52, no. 1, pp. 127–131.
- Liu, Q., Wang, A., Wang, X., and Zhang, T., *Micropor. Mesopor. Mater.*, 2006, vol. 92, nos. 1–3, pp. 10–21.  
<https://doi.org/10.1016/j.micromeso.2005.12.012>
- Kumar, M., Lal, B., Singh, A., Saxena, A.K., Dangwal, V.S., Sharma, L.D., and Dhar, G.M., *Indian J. Chem., Technol.*, vol. 8. 2001, pp. 157–161.
- Huang, B., Bartholomew, C.H., and Woodfield, B.F., *Micropor. Mesopor. Mater.*, 2013, vol. 177, pp. 37–46.  
<https://doi.org/10.1016/j.micromeso.2013.04.013>
- Semeykina, V.S., Polukhin, A.V., Lysikov, A.I., Kleymenov, A.V., Fedotov, K.V., and Parkhomchuk, E.V., *Catal. Lett.*, 2019, vol. 149, no. 2, pp. 513–521.  
<https://doi.org/10.1007/s10562-018-2646-3>
- Rhee, Y.W. and Guin, J.A., *Korean J. Chem. Eng.*, 1993, vol. 10, no. 2, pp. 112–123.  
<https://doi.org/10.1007/BF02697510>
- Ismagilov, Z.R., Shkrabina, R.A., and Koryabkina, N.A., *Ekologiya. Seriya analiticheskikh obzorov mirovoi literatury* (Ecology. Series of Analytical Reviews of World Literature), 1998, no. 50.
- Yilmaz, S., Kutmen-Kalpakli, Y., and Yilmaz, E., *Ceram. Int.*, 2009, vol. 35, no. 5, pp. 2029–2034.  
<https://doi.org/10.1016/j.ceramint.2008.11.006>
- Liu, Y., Chae, H.G., Choi, Y.H., and Kumar, S., *Ceram. Int.*, 2014, vol. 40, no. 5, pp. 6579–6587.  
<https://doi.org/10.1016/j.ceramint.2013.11.112>
- Zarezadeh-Mehrizi, M., Afshar Ebrahimi, A., and Rahimi, A., *Scientia Iranica*, 2018, vol. 25, no. 3, pp. 1434–1439.  
<https://doi.org/10.24200/sci.2018.20337>
- Bleta, R., Alphonse, P., Pin, L., Gressier, M., and Menu, M.J., *J. Colloid Interface Sci.*, 2012, vol. 367, no. 1, pp. 120–128.  
<https://doi.org/10.1016/j.jcis.2011.08.087>
- Donnet J.-B., Bansal, R.C., and Wang M.-J., *Carbon Black*, New York: Marcel Dekker, 1993.
- Romanenko, A.V. and Simonov, P.A., *Promyshlennyye kataliz v lektsiyakh* (Industrial Catalysis in Lectures), Noskov, A.S., Ed., Moscow: Kalvis, 2007.